energies

MDPI

Review

Electrochromic Electrodes with Enhanced Performance: Review of Morphology and Ion Transport Mechanism Modifications

Mahmoud H. Elshorbagy and Rehab Ramadan *

Physics Department, Faculty of Science, Minia University, Minia 61519, Egypt
* Correspondence: rehabramadan@mu.edu.eg

Abstract: The electrochromic (EC) performance of smart windows is highly dependent on the rate of ions insertion/extraction. A direct way to increase the ion exchange in EC device is to modify the structure of the EC electrodes. Structural changes also affect the electrical conduction between the transparent electrodes and the EC layers, leading to efficient smart windows. In more detail, modifying the structure of the EC electrodes results in an increase in the surface-to-volume ratio, which is combined with the increase in charge transfer reaction between the insertion and extraction of ions. The current review summarizes the enhancement in the EC performance due to the fabrication of nano/microstructures or hybrid structures on the surface of the EC electrodes to increase their surface area. Moreover, metal oxide thin films have poor electrical conduction, which leads to a high charge transport barrier. Accordingly, improving the electrical conductivity of the EC layer is considered another effective strategy to enhance the ion transport between the transparent conductor layer and the EC electrode. This behavior could be applied by combining the transition metal oxide with metallic nanoparticles or suitable organic/inorganic transparent conducting materials.

Keywords: surface-to-volume ratio; electrochromic electrodes; nano/micro-nanostructures; hybrid nanocomposites; coloration efficiency

1. Introduction

Smart windows are optoelectronic devices that control the transmission of solar radiation into buildings [1,2]. They are based on electrochromic (EC) materials, which turn from colored to transparent (bleached) states by changing the polarity of the biasing [3]. Using this application, we can control the amount of natural light passing into the building. In addition, it is used to block undesirable radiation such as ultraviolet (UV) or infrared (IR). Furthermore, it provides a better view for the buildings without losing privacy. The complementary smart windows are typically composed of two transparent conductors (TC), two EC materials and a polymer electrolyte [4,5]. Efficient smart windows require layers with a high optical modulation, chemical stability and high optical memory. The optical modulation is mainly dependent on the properties of the EC layer. They are classified electrically into two types: anodic and cathodic EC electrodes [6]. There is a wide range of materials that can be used as electrochromic layers. Among them, nickel oxide (NiO) and tungsten oxide (WO_3) thin films are the most widely used as anodic and cathodic EC electrodes, respectively.

Various physical and chemical fabrication methods have been studied to fabricate electrochromic thin films with different qualities and controlled parameters. For instance, NiO were prepared by electrodeposition [7], Prussian blue (PB) by spray pyrolysis technique [8], WO_3 by pulsed spray pyrolysis technique [9], NiO by sputtering [10] and Molybdenum trioxide (MoO_3) by sol-gel method [11]. The EC performance of compact metal oxides can be improved through different strategies. For instance, research efforts were made by modifying the morphology of the surface of the used transition metal oxide. This improvement is attributed to the increase of the ion injection into the active layer, in addition to shortening the time between the insertion and extraction of ions.

check for updates

Citation: Elshorbagy, M.H.; Ramadan, R. Electrochromic Electrodes with Enhanced Performance: Review of Morphology and Ion Transport Mechanism Modifications. *Energies* **2023**, *16*, 2327. https://doi.org/10.3390/en16052327

Academic Editor: Ioan Sarbu

Received: 25 December 2022
Revised: 19 January 2023
Accepted: 6 February 2023
Published: 28 February 2023

The fabrication of porous structures on the surface of the EC electrodes [12] or performing hybrid nanostructures [13,14] are some examples of this idea. Furthermore, compact metal oxide thin films have a poor electrical conduction, which leads to a high charge transport barrier [15] and, consequently, a low EC performance. Therefore, the EC performance of the EC electrodes can be improved by different strategies: for instance, by doping the metal oxide with metallic nanoparticles, e.g., lithium [16], zinc [17], copper [18], cobalt [19] and silver [20], or by increasing the surface of the active area through performing micro/nanostructured surface of the EC electrodes [21–24] or combining with conducting polymers such as poly(3,4-ethylenedioxythiophene) polystyrene sulfonate (PEDOT:PSS) [25] and copolymers such as PEDOT:PSS and PANI:PSS [26], 2,5-dithienyl-N-substituted-pyrrole (SNS) conjugated with 3,4-Ethylenedioxythiophene (EDOT) [27]. This combination leads to a better electrical transport between the EC electrode and the TC surface.

Due to the large advances in the performance of smart windows offered by such designs, it is important to summarize them in a review that provides a guide for researchers on this topic. One way to increase the performance of the electrochromic devices is to increase the surface to volume ratio of the electrochromic electrodes using nano/microfeatures [28–30]. The structural modification of the surfaces can be periodic, regular or random and may combine two types of materials: organic and inorganic. The hybridization of organic and inorganic materials in their nanostructure form gives a complex structure that collects the advantages of the three terms. Where the organic materials in general are easy to process and have low cost. The inorganic materials have high durability and stability, while nanofeatures increase the surface-to-volume ratio.

We collected both recent methods and structures applied to develop the EC performance of the anodic and cathodic electrodes of smart windows. We based our review on these topics considering the recent reports and high-performance results. The first part of the review summarizes some categories of nanostructured EC electrodes (random or periodic surface structures) and how they remarkably enhanced the EC performance of the electrodes. The next part presents the outstanding EC performance by combining nano/microstructures on the surface of the EC electrodes. This behavior is attributed to the increase in the surface-to-volume ratio. Finally, the hybridization of organic/inorganic materials creates new composite with custom EC properties. The combination of the organic and the inorganic material helps to mitigate the poor electrical conduction of the transition metal oxides, which leads to a high charge transport barrier. This arrangement collects the various structures, materials, and methods applied in this line to give a short compact capsule about advanced EC devices. Table 1 presents a comparison between the previously published review articles in the same field and the present work.

Table 1. Comparison between the previously published review articles and the current work.

Title of the Review Article	The Scope of the Article	Reference
Nanostructured electrochromic smart windows: traditional materials and NIR-selective plasmonic nanocrystals	Overview of current state-of-the-art conventional electrochromic materials	[31]
Nanostructured materials for electrochromic energy storage systems	Description of new active materials, distinct assembly techniques and transparent conductive electrodes used for developing a more efficient smart windows	[32]
A Brief Overview of Electrochromic Materials and Related Devices: A Nanostructured Materials Perspective	The paper discusses the causes of internal and external size effects in the process of modifying WO_3 electrochromic films using nanomaterials	[33]

Table 1. *Cont.*

Title of the Review Article	The Scope of the Article	Reference
Nanostructured inorganic electrochromic materials for light applications	Summarizes the classifications of electrochromic materials, including inorganic materials (e.g., transition metal oxides, Prussian blue, and polyoxometalates), organic materials (e.g., polymers, covalent organic frameworks, and viologens), inorganic-organic hybrids, and plasmonic materials.	[6]
Electrochromic electrodes with enhanced performance: Review of morphology and ion transport mechanism modifications	Summarize direct ways to increase the ion exchange in EC device due to modifying surface morphology and composition of the EC electrodes.	Current review

2. Strategies to Modify the Morphology of the Electrochromic Electrodes

2.1. Nanostructured Periodic Arrays

Surface texture is a method that is widely used to manage light propagation in optoelectronic devices. In smart windows, a solid electrolyte is usually casted between the two EC layers. Texturing the surface of the EC layer increases the adhesion between the solid electrolyte and the EC layer and increases the surface-to-volume ratio between them. This behavior leads to an enhancement in the coloration efficiency by increasing the amount and rate of ion injection and extraction in the device. Furthermore, this design reduces the diffusion path for the ions in a complete cycle through the device. Regular geometry that is repeated over long spatial range is called periodic nanostructure arrays. These designs are widely used in electrochromic applications to enhance the performance of the electrodes. Various geometrical shapes reveal a high coloration efficiency (CE). Core-shell structure reveals a CE of 104.6 cm^2/C, which decreased by only 11.8% after 1000 cycles [34]. Recently, hybrid core–shell-type nanostructures were used to fabricate electrochromic devices with optical modulation of 45% [35]. The obtained CE is more than 145 cm^2/C, which is retained after 1500 cycles without significant degradation. The combination of core-shell structure with nanowire applied to flexible transparent electrodes enhances the electrochemical stability and the electrochromic performance of the device [36]. A high optical modulation of 72% at 550 nm was achieved. Both electrical conductivity ($\Delta R/R \approx 8.3\%$ and 14%) and electrochromic performance (90% and 92%) maintained after 20,000 bending cycles. Moreover, the CE reaches a value of 79.49 cm^2/C. Many other nanostructured designs were applied to enhance both CE and durability by maintaining their initial performance after hundreds and thousands of cycles. Some recent examples are based on quantum dots [37], nanofibers [38], hierarchical nanostructures [39], nanorods [40], nanowires [41] and nano-flower shape structure [42]. Most of these structures can be fabricated using chemical-based techniques, which means low cost and scalable fabrication availability.

The combination between self-assembled colloidal method with electrodeposition is used to fabricated well-ordered nanoholes or nanopore NiO films [12]. Y.F. Yuan et al. studied the comparison between the electrochromic performance of compact NiO thin films and ordered porous NiO films [12]. The structure was prepared by electrodeposition using a self-assembled colloidal crystal template. The electrochromic properties were investigated in an aqueous solution of KOH (0.1 M). Figure 1a portrays the morphology of the ordered porous NiO thin film. Figure 1b shows the comparison between the optical transmittance in the colored and bleached states in the 200 to 900 nm wavelength range for the compact and the ordered porous NiO thin layers. From the reported experimental data, the optical modulation ($\Delta OD(\lambda)$) at 550 nm for the ordered porous NiO thin layer is 76% while it is only 51% for the compact one. Furthermore, Figure 1c shows the cyclic voltammetry behavior for the two structures of NiO thin films. Accordingly, the cathodic and anodic peak currents for the modified porous structure are higher than those of the compact NiO thin film. As a result, an improvement in the switching speed, optical modulation, and coloration efficiency (η) is obtained for the porous electrode, where η increased from

27 cm^2 C^{-1} for compact NiO thin films to 41 cm^2 C^{-1} for ordered porous NiO thin layer at 550 nm.

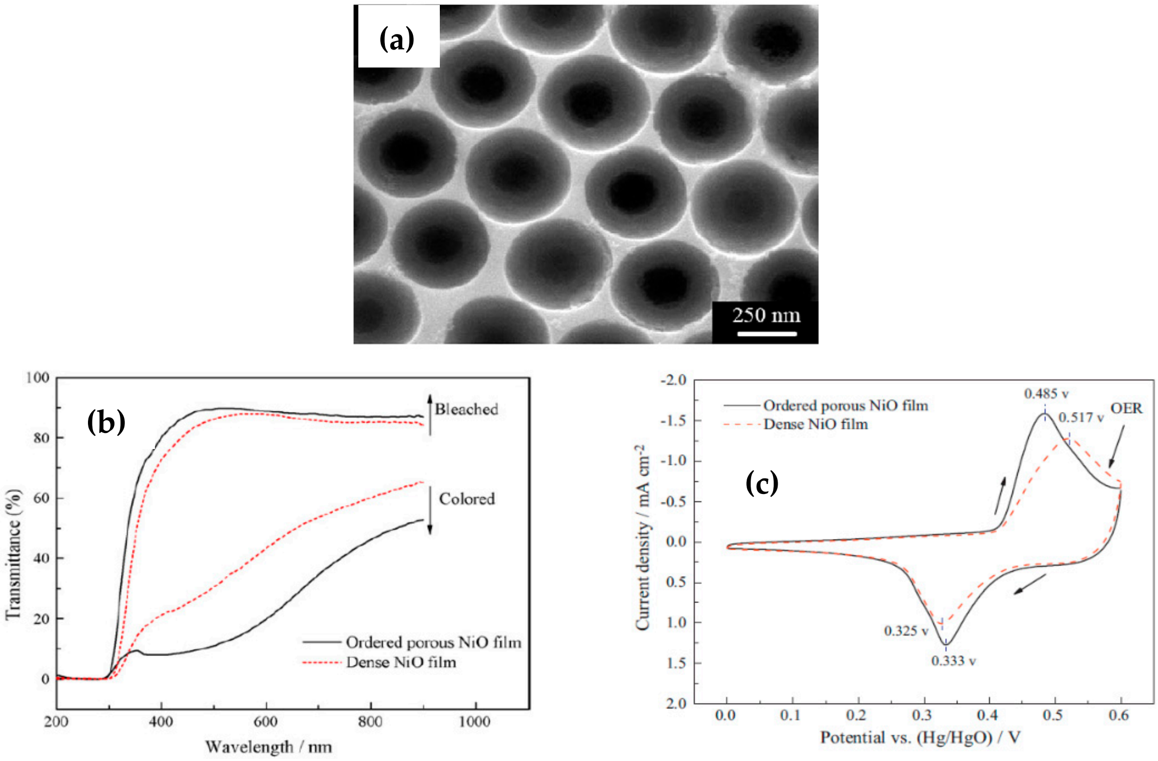

Figure 1. (**a**) Top-view FESEM image showing the morphology of the fabricated ordered porous NiO thin films. (**b**) Transmission of compact NiO thin film and ordered porous NiO thin film in the colored and bleached states. (**c**) Cyclic voltammetry for compact and ordered porous NiO thin films. Reprinted with permission (5378210053742); Copyright Year 2022, Elsevier Publisher [12].

2.2. Nanostructured Porous Surfaces

Another design of electrochromic electrodes is the random porous surfaces. In this case, the pores do not take the form of regular geometrical shapes; instead, they take homogeneous or nonhomogeneous spongy shapes. A high optical contrast of 61.4% at 633 nm wavelength was obtained for rare earth Samarium (Sm) doped WO_3 porous thin layer [43]. The nest-like porous Sm-doped WO_3 retained 91.7% of primitive optical contrast after 6000 cycles. The metal doped nanoporous structures allow the multifunctionality of the electrochromic electrodes. As an electrochromic thin film, Cu doped NiO film with assembled nanosheet structure reveals a large optical modulation (77.1% at 550 nm), short color switching time (10.6/14.3 s) and high coloration efficiency (66.3 cm^2/C) [44]. As a charge storage electrode, it has a high area specific capacitance of 94.7 mF/cm^2 at 0.2 mA/cm^2. A higher area specific capacitance was obtained when nanowire structure was combined with porous film structure [45]. A great enhancement for the CE is obtained for 3D reticular-like porous structure, which increases from 258 cm^2/C for the compact thin film structure to 534 cm^2/C for the porous structure [46].

The EC performance of TiO_2 thin films is poor when compared with NiO and WO_3. However, the modified designs of TiO_2 show a comparable performance. For example, nanostructured TiO_2 thin films were prepared as efficient electrochromic electrodes by doctor blade method [47]. Figure 2a shows the morphology of the fabricated porous TiO_2 thin film, while Figure 2b shows the transmission of the TiO_2 at 550 nm for different coloration times starting from the as deposited (curve-1) then increase the coloration time till the complete colored state (curve-6) with transmission of (T$_c$) 10%, then back again to complete bleaching (curve-7). The symmetrical cyclic voltammetry shown in Figure 2c proves the stability of insertion/extraction of Li^+ from the electrolyte. This structure results in a coloration efficiency of 33.7 $cm^2\ C^{-1}$ and fast response of 2 s.

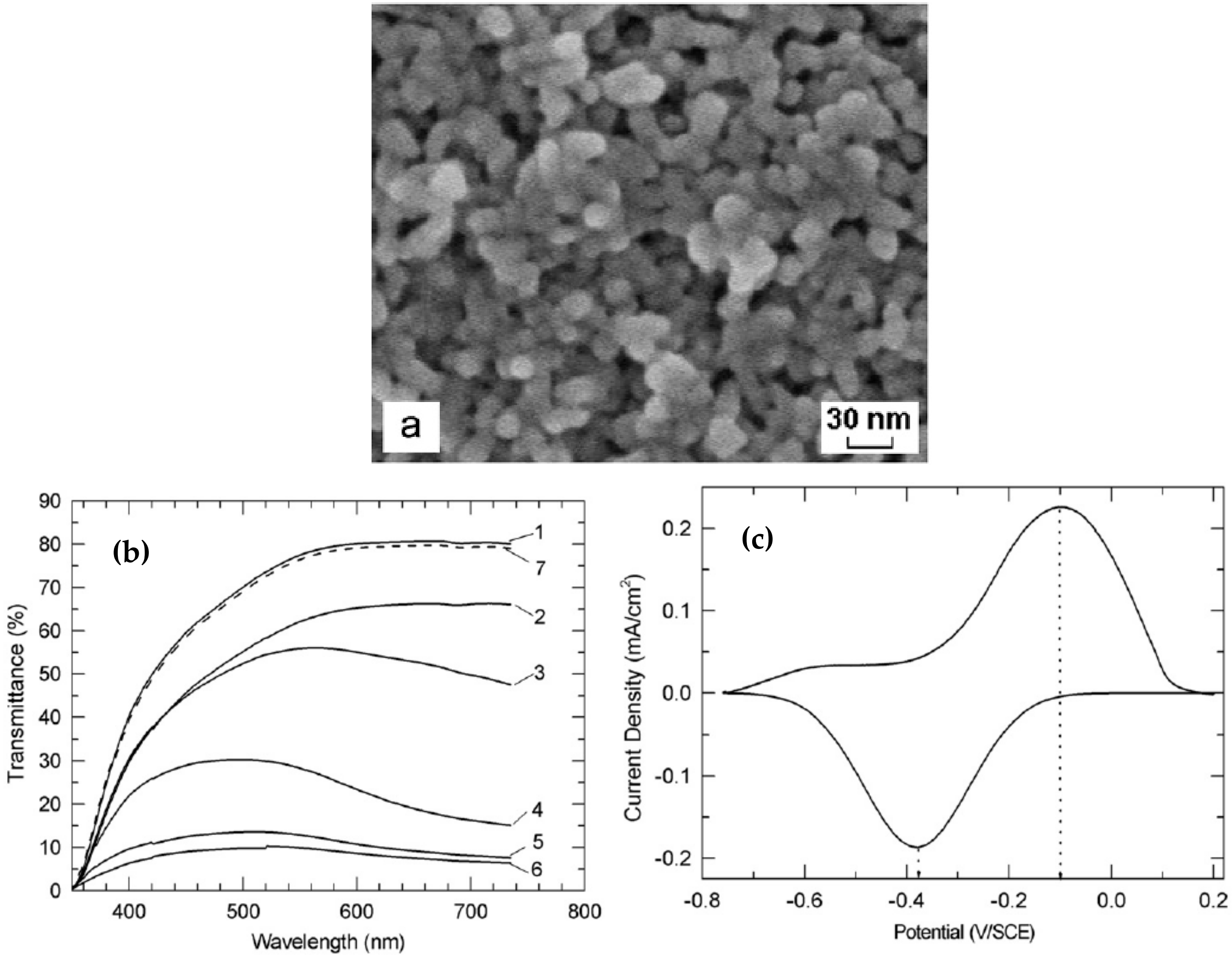

Figure 2. (**a**) Top-view FESEM image of nanostructured TiO_2 thin film. (**b**) Transmittance spectra at different states, 1- as prepared nanostructured TiO_2/FTO thin film; 2, 3, 4 and 5 are the transmittances in the colored states at coloration times of 0.5, 1, 1.5, 2, 6 s and 7 is the transmittance spectra at the bleached state. (**c**) Cyclic voltammetry of nanostructured TiO_2 thin film. Reprinted with permission (501755656); Copyright Year 2022, Elsevier Publisher [47]. Additionally, porous NiO thin films with comparable ΔOD(λ) were reported using different techniques. For instance, ΔOD(λ) was 81% using chemical bath deposition technique [48] and 80% using controlled electrodeposition technique [49]. However, compact NiO thin films usually reveal lower optical modulation. For example, pulsed laser deposition was applied to obtain crystalline NiO thin films with ΔOD(λ) of 48% [50], 38% for sol-gel processed NiO thin film [51] and 40% for sputtered one [52].

2.3. Nano/Micro Composite Surfaces

Composites involve materials with more than one phase; when processed as thin films they reveal various and tunable physical and chemical properties not likely found in monolithic thin films [53,54]. For this, composite materials with nano and micro features were extensively applied to enhance the performance of EC devices [28,55–57]. The idea is the same, increasing the surface-to-volume ratio, besides the tunable physical properties offered by the composite materials. For instance, Gözde Yurdabak Karaca et al. reported a remarkable enhancement in the EC performance of WO_3 thin films when combined with Au, poly (3, 4-ethylenedioxythiophene) (PEDOT:PSS) and Pt microtubes [14]. The resulting composite is an EC thin film with the structure WO_3/Au/PEDOT:PSS/Pt.

Figure 3 portrays the top-view and the cross-sectional views of the fabricated microtubes of Au/PEDOT:PSS/Pt composites on WO_3 thin films. Furthermore, Figure 3d,e show the spectral transmittance response for the colored and bleached states of the pure WO_3 thin film and WO_3/Au/PEDOT:PSS/Pt composite electrodes, respectively. Accordingly, the response time was shortened and the optical modulation remarkably increased for the case of WO_3/Au/PEDOT:PSS/Pt electrode. This enhancement is attributed to several reasons. First, PEDOT:PSS is a cathodic electrochromic material, so the coloration in the colored state improved, as shown in the transmittance data in Figure 3e. Furthermore, Au and Pt materials lead to enhancing the electrical conduction between the EC electrode and the TC surface. Finally, the interlinking between the microtubes and the porous structure makes the ions diffusion easier and increase the surface area for charge-transfer reactions. Accordingly, the overall electrochromic performance of the modified WO_3/Au/PEDOT:PSS/Pt structure was enhanced. The coloration and bleaching response time (t_C and t_b) of WO_3/Au/PEDOT:PSS/Pt electrode are $t_{C\,=}$ 25.86 s and $t_{b\,=}$ 15.93 s, compared with $t_{C\,=}$ 19.25 s and $t_{b\,=}$ 13.83 s for the pure WO_3 electrode. Moreover, $\Delta OD(\lambda)$ of the WO_3/Au/PEDOT:PSS/Pt composite improved from 21.9% to 26% at ±2 V.

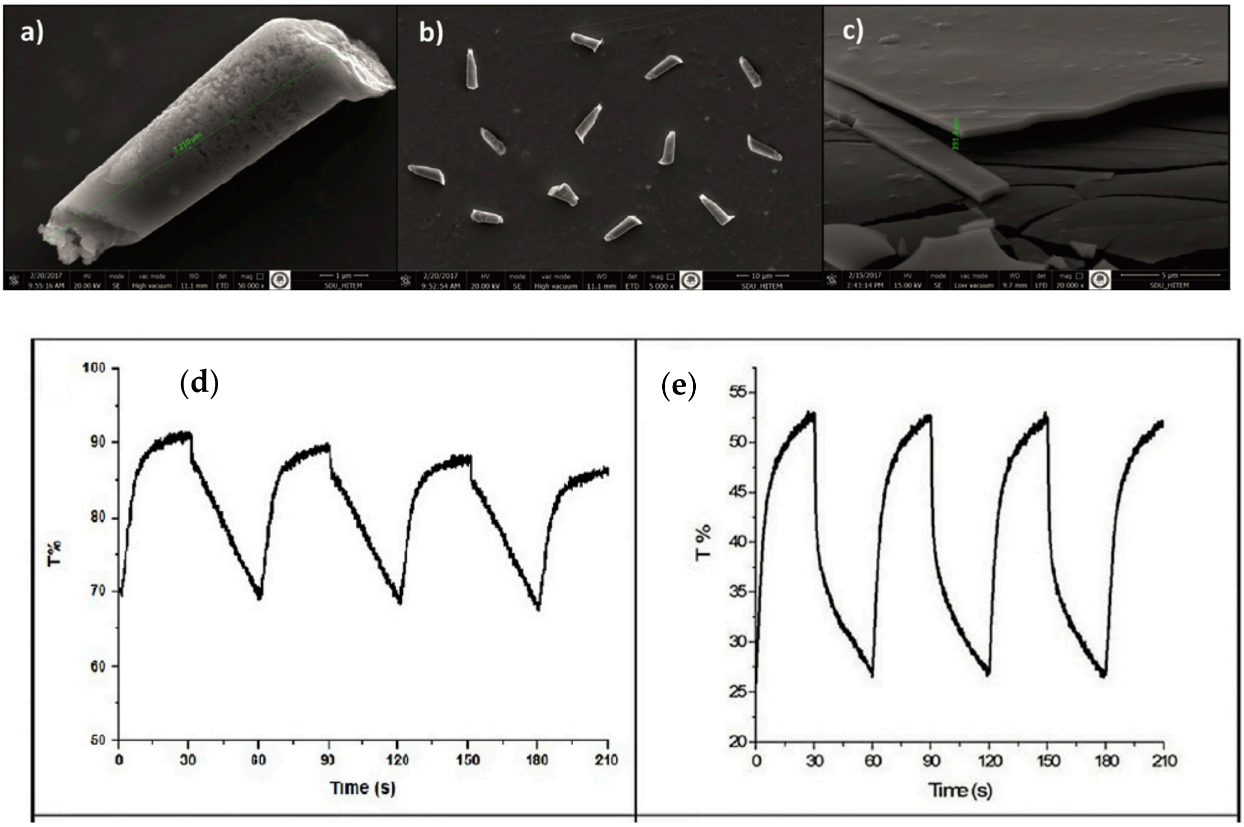

Figure 3. Typical FESEM images and spectral transmittance of WO_3 and WO_3/Au/PEDOT:PSS/Pt EC thin films. (**a**) Magnified image showing the dimensions of Au/PEDOT:PSS/Pt microtube. (**b**) Top-view image showing the distribution of the microtubes on the surface of WO_3 thin film. (**c**) Cross-sectional view of the WO_3 thin film. (**d**) Transmittance response between coloring and bleaching of WO_3 thin film. (**e**) Transmittance response between coloring and bleaching of WO_3/Au/PEDOT:PSS/Pt EC thin films. Reprinted with permission (5378140815476); Copyright Year 2022, Elsevier Publisher [14].

Moreover, Mudaliar Mahesh Margoni et al. fabricated an EC electrode of nano/microstructures of V_2O_5 in the form of nanorods accumulated with microspheres by hydrothermal method [58]. The samples show a high transmittance (maximum average is 77%) and low resistivity (minimum is 7.9×10^{-4} Ω.cm). These enhanced optical and electrical properties reveal maximum cathodic peak current as 1.8 mA/cm^2 and a maximum anodic peak current as 2.8 mA/cm^2. Furthermore, the ion diffusion coefficient was also enhanced, which makes the structure suitable for electrochromic applications. From another perspective, Md Rakibuddin et.al synthesized micro-nanostructure sized tungsten trioxide (WO_3) by thermal annealing of tungsten powder under ambient conditions [59]. The fabricated samples show a high crystallinity. Furthermore, they can tune the size of the WO_3 particles from microscale to nanoscale using the annealing temperature. The powder is then spin coated on FTO glass to obtain the EC electrode. The performance of the EC device based on the fabricated layers was compared with a device based on commercial WO_3. The coloration efficiency enhanced from 30.45 cm^2 C^{-1} for the device with the commercial layer to 32.3 cm^2 C^{-1} for the device with the fabricated WO_3 layer. An optimized electrochromic device based on this micro-nano WO_3 layer may result in a better coloration efficiency.

2.4. Hybrid Organic-Inorganic Nanocomposite EC Surfaces with Nanofeature

Organic materials are widely applied in optoelectronics, as they are, in general, solution-processed and low cost [60,61]. Despite the enhancement in the CE of organic materials, low durability due to its degradation is a general feature [62]. The idea of hybridization between organic and inorganic electrochromic layers with nanofeatures takes advantage of the three of them [63–66]. This allows the production of high-performance, low cost and long-cyclic stability EC devices [67,68]. Haizeng Li et al. recently studied the electrochromic properties of organic-inorganic nanocomposite film [25]. The film is composed of inorganic material (porous layers of tungsten molybdenum oxide nanorods $W_{0.71}Mo_{0.29}O_3$) permeated with an interconnected conductive organic layer of PEDOT:PSS. In the reported study, the EC properties of the conjugated polymer of $W_{0.71}Mo_{0.29}O_3$/PEDOT:PSS were compared with the $W_{0.71}Mo_{0.29}O_3$ and PEDOT:PSS alone. The purpose of the combination between the organic and the inorganic material is to mitigate the poor electrical conduction of the transition metal oxides, which leads to a high charge transport barrier. Figure 4a shows the typical morphology of the fabricated porous $W_{0.71}Mo_{0.29}O_3$ electrode, while Figure 4b portrays the morphology of the nanocomposite after the growth of the PEDOT:PSS layer. Filling in the pores of porous $W_{0.71}Mo_{0.29}O_3$ electrode with PEDOT:PSS leads to increasing the pathway for charge transportation. This behavior is expected to decrease the charge transport barrier and enhance the electrochromic performance. Figure 4c shows the optical behavior of the hybrid organic-inorganic EC electrode in the colored and bleached states at ±1 V in 1 M $LiClO_4$-propyline carbonate solution. The optical contrast of the mixed composite is 65.1% at 632.8 nm, which is higher than both $W_{0.71}Mo_{0.29}O_3$ (54.5%) and PEDOT:PSS electrode (51.4%). Furthermore, Figure 4d summarizes the switching response between coloring and bleaching of $W_{0.71}Mo_{0.29}O_3$ electrode, PEDOT:PSS electrode and hybrid $W_{0.71}Mo_{0.29}O_3$/PEDOT:PSS for the hybrid $W_{0.71}Mo_{0.29}O_3$/PEDOT:PSS electrode, which is given as t_c = 17.9 s, t_b = 10.5 s compared with t_c = 22.1 s and t_b = 13.9 s for $W_{0.71}Mo_{0.29}O_3$ electrode. This response is attributed to the high electrical conduction of PEDOT:PSS layer, which promotes the charge transfer efficiency by providing more active areas in $W_{0.71}Mo_{0.29}O_3$ to interact with Li^+ in the electrolyte, while, PEDOT:PSS electrode gives the fastest response (t_c = 6.5 s, t_b = 3 s) as a result of its high electrical conduction. Accordingly, the coloration efficiency of the hybrid $W_{0.71}Mo_{0.29}O_3$/PEDOT:PSS electrode is 52.8 cm^2 C^{-1}, twice more than that of $W_{0.71}Mo_{0.29}O_3$ electrode (21.7 cm^2 C^{-1}).

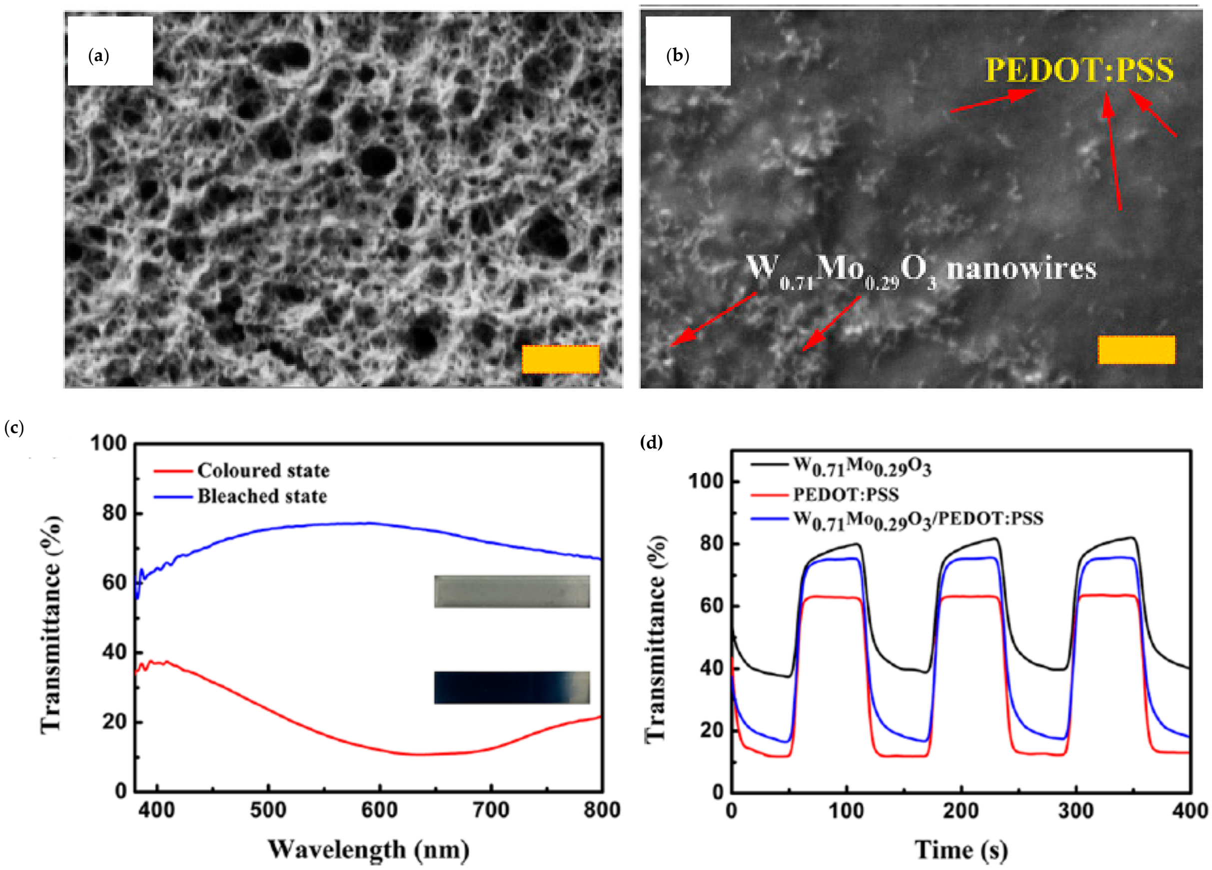

Figure 4. (**a**) Typical top-view FESEM image of porous $W_{0.71}Mo_{0.29}O_3$ electrode. (**b**) Typical top-view image of $W_{0.71}Mo_{0.29}O_3$/PEDOT:PSS electrode showing the composition of the nanocomposite. (**c**) Optical transmittance of $W_{0.71}Mo_{0.29}O_3$/PEDOT:PSS electrode in the colored and bleached states at ±1 V in 1 M $LiClO_4$-propyline carbonate solution. (**d**) Switching between colored and bleached states for the three electrodes at 632.8 nm [25].

Hybrid nanostructures of PEDOT:PSS and graphene oxide (GO) layer are another example of hybrid nanocomposites leading to enhancing the electrochromic performance of smart windows. Yingdi Shi et al. studied the effect of combining GO nanosheet with PEDOT:PSS EC thin film through the electro-polymerization method [30]. Figure 5a shows the morphology of the pristine PEDOT:PSS layer and Figure 5b shows the morphology after the growth of the GO nanosheet. The FESEM image of PEDOT:PSS layer shows the formation of a rough surface with a high surface area, which favors deeper ion injection into the active layer. Figure 5c,d show the optical behavior for pristine PEDOT:PSS and hybrid PEDOT:PSS/GO nanostructures from 300 nm to 800 nm wavelength range, respectively. Accordingly, the optical contrast between coloring and bleaching increased from 23.4% to 34.4% after the hybridization with GO nanosheet at 480 nm, in addition to shortening the coloring and bleaching time from 1800 ms to 300 ms and 1500 ms to 400 ms, respectively. Moreover, the coloration efficiency improved from 53.5 $cm^2\ C^{-1}$ to 64.9 $cm^2\ C^{-1}$ due to the hybridization with the GO layer. This enhancement in the EC performance of the hybrid PEDOT:PSS/GO nanostructured electrode is attributed to the increase in the surface-to-volume ratio of PEDOT:PSS layer. In addition, the growth of GO nanosheet functionalized the surface of the PEDOT:PSS layer and contributed as a buffer layer.

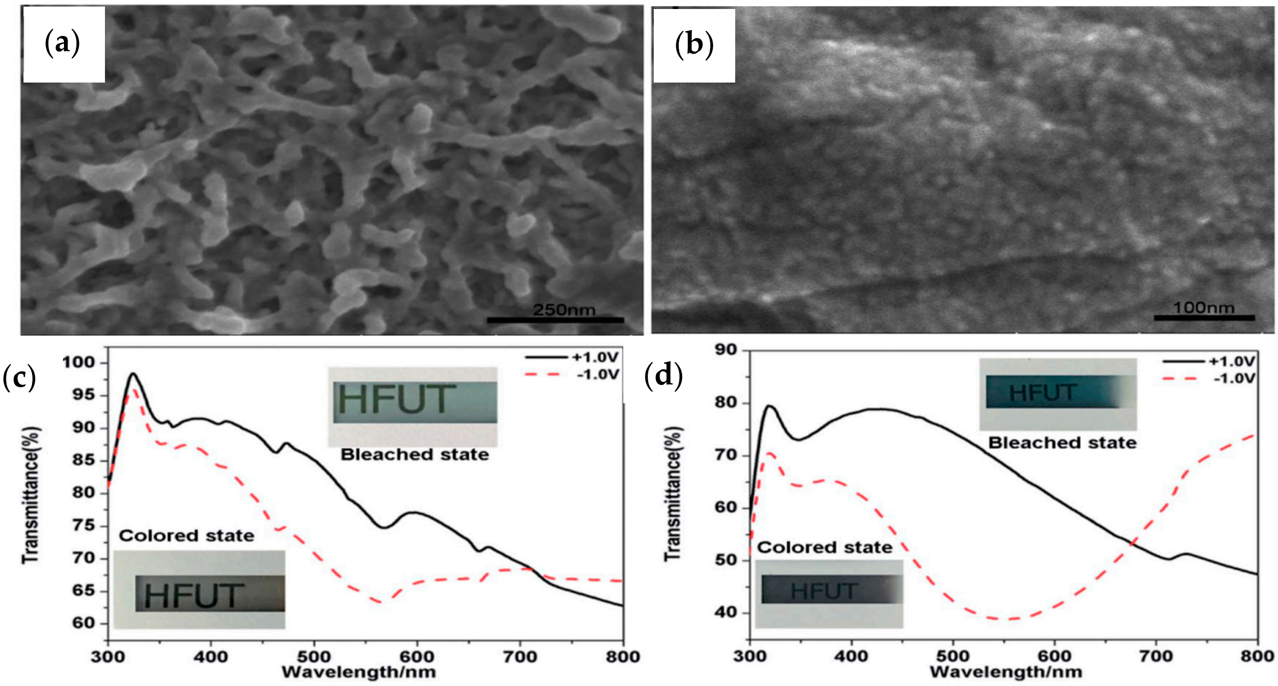

Figure 5. (**a**) Typical FESEM image of pristine PEDOT:PSS, layer. (**b**) Typical FESEM image of hybrid PEDOT:PSS/GO nanostructures. (**c**) Spectral transmittance of PEDOT:PSS layer in the colored and bleached states at ± 1 V. (**d**) Spectral transmittance of hybrid PEDOT:PSS/GO layer in the colored and bleached states at ±1 V [30].

According to the results presented in the current review, we predict better EC performance of smart windows because of improving ion insertions and extractions through the fabrication of nanostructured EC electrodes or hybrid nanostructures on its surface. So far, we are thinking of combining the increase in the surface-to-volume ratio by texturing the surface of the EC electrodes and improving the electrical conduction of the transparent electrodes. The first increases the total ion transfer through the device and the second enhances the rate of this transfer, which in turn leads to high optical contrast and fast switching time. The next focus of research may be on applying hybrid organic/inorganic materials in their nano or microforms to the different layers of the device. These combinations involve wide options and selections in both materials and designs that need to be explored through future research.

3. Conclusions

The results provided in the current review summarize some of the remarkable enhancements in the performance of the electrochromic devices due to modifying the surface of the working and counter EC electrodes of smart windows. The reported modification methods are concluded in three points:

1. Texturing the EC electrode surface, the implementation of nano/microstructures or hybrid nanostructures on the surface of the EC electrode led to the increase in the surface-to-volume ratio.
2. The incorporation with metallic nanoparticles (e.g., Au or Pt) leads to improving the electrical conduction between the electrochromic electrode and the transparent conductor surface.
3. The combination with organic transparent conductors (e.g., PEDOT:PSS or PANI:PSS) results in improving the electrical conduction in addition to decreasing the time between insertion and extraction of ions.

Generally, the enhancement in the electrochromic properties of the electrochromic electrodes by the mentioned methods can contribute remarkably to the production of efficient smart window applications. For instance, Y.F. Yuan et al. studied the comparison between the electrochromic performance of compact NiO thin films and ordered porous NiO films, where the efficiency increased from 27 cm^2 C^{-1} for dense NiO thin films to 41 cm^2 C^{-1} for ordered porous NiO thin films at 550 nm. Moreover, the fabrication of nanostructured TiO_2 thin films results in a coloration efficiency of 33.7 cm^2 C^{-1} and a fast response of 2 s. From another perspective, Gözde Yurdabak Karaca et al. reported on the remarkable enhancement in the electrochromic performance of WO_3 thin films due to the combination with Au, poly (3, 4-ethylenedioxythiophene) (PEDOT:PSS) and Pt microtubes, where coloration efficiency enhanced from 30.45 cm^2 C^{-1} for the device with the WO_3 thin film to 32.3 cm^2 C^{-1} for the modified one. In addition, Yingdi Shi et al. reported an enhancement in the coloration efficiency from 53.5 cm^2 C^{-1} to 64.9 cm^2 C^{-1} due to combining PEDOT:PSS thin film with graphene oxide nanosheet. According to the results presented in the current review, we predict better EC performance of smart windows because of improving ion insertions and extractions through the fabrication of nanostructured EC electrodes or hybrid nanostructures on their surface.

Author Contributions: Conceptualization, R.R. and M.H.E.; validation, R.R. and M.H.E.; writing—original draft preparation, R.R. and M.H.E.; writing—review and editing, R.R. and M.H.E.; visualization, R.R. and M.H.E.; supervision, R.R. and M.H.E.; project administration, R.R. and M.H.E.; funding acquisition, R.R. and M.H.E. All authors have read and agreed to the published version of the manuscript.

Funding: This research received no external funding.

Data Availability Statement: Not applicable.

Acknowledgments: R. Ramadan. and M. H. Elshorbagy are thankful to the journal *Energies* for their invitation to publish this work free of charge.

Conflicts of Interest: The authors declare no conflict of interest.

References

1. Baetens, R.; Jelle, B.P.; Gustavsen, A. Properties, requirements and possibilities of smart windows for dynamic daylight and solar energy control in buildings: A state-of-the-art review. *Sol. Energy Mater. Sol. Cells* **2010**, *94*, 87–105. [CrossRef]
2. Casini, M. Smart windows for energy efficiency of buildings. In Proceedings of the Second International Conference on Advances in Civil, Structural and Environmental Engineering–ACSEE, Zürich, Switzerland, 25–26 October 2014; pp. 273–281.
3. Granqvist, C.; Azens, A.; Hjelm, A.; Kullman, L.; Niklasson, G.A.; Rönnow, D.; Mattsson, M.S.; Veszelei, M.; Vaivars, G. Recent advances in electrochromics for smart windows applications. *Sol. Energy* **1998**, *63*, 199–216. [CrossRef]
4. Ramadan, R.; Kamal, H.; Hashem, H.; Abdel-Hady, K. Gelatin-based solid electrolyte releasing Li+ for smart window applications. *Sol. Energy Mater. Sol. Cells* **2014**, *127*, 147–156. [CrossRef]
5. Ramadan, R.; Elshorbagy, M.; Kamal, H.; Hashem, H.; Abdelhady, K. Preparation and characterization of protonic solid electrolyte applied to a smart window device with high optical modulation. *Optik* **2017**, *135*, 85–97. [CrossRef]
6. Zhang, W.; Li, H.; Hopmann, E.; Elezzabi, A.Y. Nanostructured inorganic electrochromic materials for light applications. *Nanophotonics* **2021**, *10*, 825–850. [CrossRef]
7. Sonavane, A.; Inamdar, A.; Shinde, P.; Deshmukh, H.; Patil, R.; Patil, P. Efficient electrochromic nickel oxide thin films by electrodeposition. *J. Alloys Compd.* **2010**, *489*, 667–673. [CrossRef]
8. Elshorbagy, M.; Ramadan, R.; Abdelhady, K. Preparation and characterization of spray-deposited efficient Prussian blue electrochromic thin film. *Optik* **2017**, *129*, 130–139. [CrossRef]
9. Bathe, S.R.; Patil, P. Electrochromic characteristics of fibrous reticulated WO_3 thin films prepared by pulsed spray pyrolysis technique. *Sol. Energy Mater. Sol. Cells* **2007**, *91*, 1097–1101. [CrossRef]
10. Yoshimura, K.; Miki, T.; Tanemura, S.T.S. Nickel oxide electrochromic thin films prepared by reactive DC magnetron sputtering. *Jpn. J. Appl. Phys.* **1995**, *34*, 2440. [CrossRef]
11. Lin, S.-Y.; Wang, C.-M.; Kao, K.-S.; Chen, Y.-C.; Liu, C.-C. Electrochromic properties of MoO_3 thin films derived by a sol–gel process. *J. Sol-Gel Sci. Technol.* **2010**, *53*, 51–58. [CrossRef]
12. Yuan, Y.; Xia, X.; Wu, J.; Chen, Y.; Yang, J.; Guo, S. Enhanced electrochromic properties of ordered porous nickel oxide thin film prepared by self-assembled colloidal crystal template-assisted electrodeposition. *Electrochim. Acta* **2011**, *56*, 1208–1212. [CrossRef]
13. Popov, A.; Brasiunas, B.; Damaskaite, A.; Plikusiene, I.; Ramanavicius, A.; Ramanaviciene, A. Electrodeposited gold nanostructures for the enhancement of electrochromic properties of PANI–PEDOT film deposited on transparent electrode. *Polymers* **2020**, *12*, 2778. [CrossRef] [PubMed]

14. Karaca, G.Y.; Eren, E.; Cogal, G.C.; Uygun, E.; Oksuz, L.; Oksuz, A.U. Enhanced electrochromic characteristics induced by Au/PEDOT/Pt microtubes in WO_3 based electrochromic devices. *Opt. Mater.* **2019**, *88*, 472–478. [CrossRef]
15. Rao, T.; Zhou, Y.; Jiang, J.; Yang, P.; Liao, W. Low Dimensional Transition Metal Oxide towards Advanced Electrochromic Devices. *Nano Energy* **2022**, *100*, 107479. [CrossRef]
16. Chang, J.-Y.; Chen, Y.-C.; Wang, C.-M.; Chen, Y.-W. Electrochromic properties of Li-doped NiO films prepared by RF magnetron sputtering. *Coatings* **2020**, *10*, 87. [CrossRef]
17. Kim, K.H.; Kahuku, M.; Abe, Y.; Kawamura, M.; Kiba, T. Improved electrochromic performance in nickel oxide thin film by Zn doping. *Int. J. Electrochem. Sci* **2020**, *15*, 4065–4071. [CrossRef]
18. Kim, K.H.; Takahashi, C.; Abe, Y.; Kawamura, M. Effects of Cu doping on nickel oxide thin film prepared by sol–gel solution process. *Optik* **2014**, *125*, 2899–2901. [CrossRef]
19. Kim, K.H.; Fujii, S.; Abe, Y. Incorporation of Co^{2+}, Cu^{2+}, and Zn^{2+} ions into nickel oxide thin films and their enhanced electrochemical and electrochromic performances. *Int. J. Electrochem. Sci.* **2022**, *17*, 220125. [CrossRef]
20. Deonikar, V.G.; Puguan, J.M.C.; Kim, H. Ag nanoparticles embedded defective tungsten oxide hydrate thin films for the enhanced electrochromic performance: Insights on the physico-chemical properties and localized surface plasmon resonance mechanism. *Acta Mater.* **2021**, *207*, 116693. [CrossRef]
21. Ezhilmaran, B.; Bhat, S.V. Enhanced charge transfer in TiO_2 nanoparticles/MoO_3 nanostructures bilayer heterojunction electrode for efficient electrochromism. *Mater. Today Commun.* **2022**, *31*, 103497. [CrossRef]
22. Klein, J.; Hein, A.; Bold, E.; Alarslan, F.; Oesterschulze, E.; Haase, M. Intercalation-free, fast switching of mesoporous antimony doped tin oxide with cathodically coloring electrochromic dyes. *Nanoscale Adv.* **2022**, *4*, 2144–2152. [CrossRef] [PubMed]
23. Reddy, G.A.; Shaik, H.; Kumar, K.N.; Shetty, H.D.; Jafri, R.I.; Naik, R.; Gupta, J.; Sattar, S.A.; Doreswamy, B. Synthesis, characterizations, and electrochromic studies of WO_3 coated CeO_2 nanorod thin films for smart window applications. *Phys. B Condens. Matter* **2022**, *647*, 414395. [CrossRef]
24. Wang, L.; Liu, Y.; Han, G.; Zhao, H. Dual-band electrochromic film based on mesoporous h-WO_3/o-$WO_3 \cdot H_2O$/r-TiO_2 for high performance smart windows. *Sol. Energy Mater. Sol. Cells* **2023**, *250*, 112053. [CrossRef]
25. Li, H.; McRae, L.; Elezzabi, A.Y. Solution-processed interfacial PEDOT: PSS assembly into porous tungsten molybdenum oxide nanocomposite films for electrochromic applications. *ACS Appl. Mater. Interfaces* **2018**, *10*, 10520–10527. [CrossRef] [PubMed]
26. Park, C.; Kim, J.M.; Kim, Y.; Bae, S.; Do, M.; Im, S.; Yoo, S.; Kim, J.H. High-Coloration Efficiency and Low-Power Consumption Electrochromic Film based on Multifunctional Conducting Polymer for Large Scale Smart Windows. *ACS Appl. Electron. Mater.* **2021**, *3*, 4781–4792. [CrossRef]
27. Ergun, E.G.C.; Carbas, B.B. Electrochromic copolymers of 2,5-dithienyl-N-substituted-pyrrole (SNS) derivatives with EDOT: Properties and electrochromic device applications. *Mater. Today Commun.* **2022**, *32*, 103888. [CrossRef]
28. Mallikarjuna, K.; Shinde, M.A.; Kim, H. Electrochromic smart windows using 2D-MoS_2 nanostructures protected silver nanowire based flexible transparent electrodes. *Mater. Sci. Semicond. Process.* **2020**, *117*, 105176. [CrossRef]
29. Mendieta-Reyes, N.E.; Díaz-García, A.K.; Gómez, R. Simultaneous electrocatalytic CO_2 reduction and enhanced electrochromic effect at WO_3 nanostructured electrodes in acetonitrile. *ACS Catal.* **2018**, *8*, 1903–1912. [CrossRef]
30. Shi, Y.; Zhang, Y.; Tang, K.; Song, Y.; Cui, J.; Shu, X.; Wang, Y.; Liu, J.; Wu, Y. In situ growth of PEDOT/graphene oxide nanostructures with enhanced electrochromic performance. *RSC Adv.* **2018**, *8*, 13679–13685. [CrossRef]
31. Runnerstrom, E.L.; Llordés, A.; Lounis, S.D.; Milliron, D.J. Nanostructured electrochromic smart windows: Traditional materials and NIR-selective plasmonic nanocrystals. *Chem. Commun.* **2014**, *50*, 10555–10572. [CrossRef]
32. Dalavi, D.S.; Desai, R.S.; Patil, P.S. Nanostructured materials for electrochromic energy storage systems. *J. Mater. Chem. A* **2022**, *10*, 1179–1226. [CrossRef]
33. Shchegolkov, A.V.; Jang, S.-H.; Shchegolkov, A.V.; Rodionov, Y.V.; Sukhova, A.O.; Lipkin, M.S. A brief overview of electrochromic materials and related devices: A nanostructured materials perspective. *Nanomaterials* **2021**, *11*, 2376. [CrossRef] [PubMed]
34. Wang, Y.; Gong, Z.; Zeng, Y.; Zhao, H.; Yang, J. High-Properties electrochromic device based on TiO_2@ Graphene/Prussian blue Core-Shell nanostructures. *Chem. Eng. J.* **2022**, *431*, 134066. [CrossRef]
35. Mishra, S.; Lambora, S.; Yogi, P.; Sagdeo, P.R.; Kumar, R. Organic nanostructures on inorganic ones: An efficient electrochromic display by design. *ACS Appl. Nano Mater.* **2018**, *1*, 3715–3723. [CrossRef]
36. Hao, T.; Wang, S.; Xu, H.; Zhang, X.; Xue, J.; Liu, S.; Song, Y.; Li, Y.; Zhao, J. Stretchable electrochromic devices based on embedded WO_3@ AgNW Core-Shell nanowire elastic conductors. *Chem. Eng. J.* **2021**, *426*, 130840. [CrossRef]
37. Ahmad, K.; Song, G.; Kim, H. Fabrication of Tungsten Oxide/Graphene Quantum Dot (WO_3@ GQD) Thin Films on Indium Tin Oxide-Based Glass and Flexible Substrates for the Construction of Electrochromic Devices for Smart Window Applications. *ACS Sustain. Chem. Eng.* **2022**, *10*, 11948–11957. [CrossRef]
38. Zhang, S.; Chen, S.; Yang, F.; Hu, F.; Yan, B.; Gu, Y.; Jiang, H.; Cao, Y.; Xiang, M. High-performance electrochromic device based on novel polyaniline nanofibers wrapped antimony-doped tin oxide/TiO_2 nanorods. *Org. Electron.* **2019**, *65*, 341–348. [CrossRef]
39. Hu, F.; Yan, B.; Ren, E.; Gu, Y.; Lin, S.; Ye, L.; Chen, S.; Zeng, H. Constructing spraying-processed complementary smart windows via electrochromic materials with hierarchical nanostructures. *J. Mater. Chem. C* **2019**, *7*, 14855–14860. [CrossRef]
40. Duan, Y.; Wang, C.; Hao, J.; Jiao, Y.; Xu, Y.; Wang, J. Electrochromic Performance and Capacitor Performance of α-MoO_3 Nanorods Fabricated by a One-Step Procedure. *Coatings* **2021**, *11*, 783. [CrossRef]

41. Shinde, M.A.; Kim, H. Highly stable silver nanowire-based transparent conductive electrodes for electrochromic devices. *Mater. Today Commun.* **2021**, *26*, 102147. [CrossRef]
42. Kandpal, S.; Ghosh, T.; Rani, C.; Rani, S.; Pathak, D.K.; Tanwar, M.; Bhatia, R.; Sameera, I.; Kumar, R. MoS_2 nano-flower incorporation for improving organic-organic solid state electrochromic device performance. *Sol. Energy Mater. Sol. Cells* **2022**, *236*, 111502. [CrossRef]
43. Xie, H.; Wang, Y.; Liu, H.; Wang, H.; Li, Y.; Qi, X.; Liang, T.; Zeng, J. Electrochromic electrode with high optical contrast and long cyclic life using nest-like porous doped-Sm WO_3 films. *Ceram. Int.* **2023**, *49*, 8223. [CrossRef]
44. Wang, J.; Huo, X.; Yan, F.; Wang, H.; Zhang, M.; Guo, M. Lamella self-assembled Cu-doped NiO nanosheet arrays for dual-function devices with balanced electrochromic and energy storage performance. *Appl. Surf. Sci.* **2022**, *604*, 154504. [CrossRef]
45. Zhang, M.; Xu, X.; Gu, Y.; Cheng, X.; Hu, J.; Xiong, K.; Jiang, Y.; Fan, T.; Xu, J. Porous and nanowire-structured NiO/AgNWs composite electrodes for significantly-enhanced supercapacitive and electrochromic performances. *Nanotechnology* **2021**, *32*, 275405. [CrossRef]
46. Zhang, W.; Wang, X.; Wang, S.; Zhu, S.; Wang, Q. Morphology and electrochromic properties of nanostructured polyterthiophene films formed by different deposition modes. *Sol. Energy Mater. Sol. Cells* **2021**, *230*, 111269. [CrossRef]
47. Dinh, N.N.; Quyen, N.M.; Zikova, M.; Truong, V.-V. Highly-efficient electrochromic performance of nanostructured TiO_2 films made by doctor blade technique. *Sol. Energy Mater. Sol. Cells* **2011**, *95*, 618–623. [CrossRef]
48. Xia, X.; Tu, J.; Zhang, J.; Wang, X.; Zhang, W.; Huang, H. Electrochromic properties of porous NiO thin films prepared by a chemical bath deposition. *Sol. Energy Mater. Sol. Cells* **2008**, *92*, 628–633. [CrossRef]
49. Wu, M.-S.; Yang, C.-H.; Wang, M.-J. Morphological and structural studies of nanoporous nickel oxide films fabricated by anodic electrochemical deposition techniques. *Electrochim. Acta* **2008**, *54*, 155–161. [CrossRef]
50. Bouessay, I.; Rougier, A.; Poizot, P.; Moscovici, J.; Michalowicz, A.; Tarascon, J.-M. Electrochromic degradation in nickel oxide thin film: A self-discharge and dissolution phenomenon. *Electrochim. Acta* **2005**, *50*, 3737–3745. [CrossRef]
51. Sharma, P.K.; Fantini, M.; Gorenstein, A. Synthesis, characterization and electrochromic properties of NiO_xH_y thin film prepared by a sol–gel method. *Solid State Ion.* **1998**, *113*, 457–463. [CrossRef]
52. Ferreira, F.; Tabacniks, M.; Fantini, M.; Faria, I.; Gorenstein, A. Electrochromic nickel oxide thin films deposited under different sputtering conditions. *Solid State Ion.* **1996**, *86*, 971–976. [CrossRef]
53. Ramadan, R.; Torres-Costa, V.; Martín-Palma, R.J. Fabrication of Zinc Oxide and Nanostructured Porous Silicon Composite Micropatterns on Silicon. *Coatings* **2020**, *10*, 529. [CrossRef]
54. Ramadan, R.; Dadgostar, S.; Manso–Silván, M.; Pérez-Casero, R.; Hernandez-Velez, M.; Jimenez, J.; Sanchez, O. Silver-enriched ZnO: Ag thin films deposited by magnetron co-sputtering: Post annealing effects on structural and physical properties. *Mater. Sci. Eng. B* **2022**, *276*, 115558. [CrossRef]
55. Pan, J.; Zheng, R.; Wang, Y.; Ye, X.; Wan, Z.; Jia, C.; Weng, X.; Xie, J.; Deng, L. A high-performance electrochromic device assembled with hexagonal WO_3 and NiO/PB composite nanosheet electrodes towards energy storage smart window. *Sol. Energy Mater. Sol. Cells* **2020**, *207*, 110337. [CrossRef]
56. Prasad, A.K.; Park, J.-Y.; Jung, H.Y.; Kang, J.W.; Kang, S.-H.; Ahn, K.-S. Electrochemical deposition of Ni-WO_3 thin-film composites for electrochromic energy storage applications: Novel approach toward quantum-dot-sensitized solar cell-assisted Ni-WO_3 electrochromic device. *J. Ind. Eng. Chem.* **2023**, *117*, 500–509. [CrossRef]
57. Sharma, R.; Sharma, M.; Goswamy, J. Synthesis and characterization of MoS_2/WO_3 nanocomposite for electrochromic device application. *Int. J. Energy Res.* **2022**, *46*, 22176–22187. [CrossRef]
58. Margoni, M.M.; Mathuri, S.; Ramamurthi, K.; Babu, R.R.; Ganesh, V.; Sethuraman, K. Hydrothermally grown nano and microstructured V_2O_5 thin films for electrochromic application. *Appl. Surf. Sci.* **2018**, *449*, 193–202. [CrossRef]
59. Rakibuddin, M.; Kim, H. Synthesis and characterization of facile industrially scalable and cost effective WO_3 micro–nanostructures for electrochromic devices and photocatalyst. *Ceram. Int.* **2018**, *44*, 16615–16623. [CrossRef]
60. Lee, K.; Han, M.; Kwon, G.; Jeon, Y.; Kim, J.; You, J. A facile nanoarghitectonics of electrochromic devices with poly (3,4-ethylenedioxythiophene) and bioplastic composite. *Appl. Surf. Sci.* **2022**, *613*, 155955. [CrossRef]
61. Lin, K.; Chen, H.; Liang, H.; Tan, J.; Zhou, D.; Zhang, X.; Liu, F.; Wang, Y. Benzotriazole-EDOT electrochromic conjugated polymers show sub-second response time and 774 $cm^2\ C^{-1}$ coloration efficiency. *New J. Chem.* **2022**, *46*, 16684–16692. [CrossRef]
62. Halder, S.; Behere, R.P.; Gupta, N.; Kuila, B.K.; Chakraborty, C. Enhancement of the electrochemical performance of a cathodically coloured organic electrochromic material through the formation of hydrogen bonded supramolecular polymer assembly. *Sol. Energy Mater. Sol. Cells* **2022**, *245*, 111858. [CrossRef]
63. Li, Q.; Wang, B.; Zou, H.; Guo, Q.; Nie, G. High performance multi-color prussian blue/poly (indole-5-carboxylic acid) nanocomposites with multiple layer nanosphere structure for electrochromic supercapacitor application. *J. Alloys Compd.* **2022**, *921*, 166140. [CrossRef]
64. Wang, P.; Sun, Y.; Li, J.; Zhu, G.; Zhang, X.; Yang, H.; Lin, B. A novel p/n-dopable electrochromic electrode material based on P (TPACz)/WO_3 coralloid porous nanocomposite. *J. Alloys Compd.* **2022**, *922*, 166195. [CrossRef]
65. Roy, S.; Ganeshan, S.K.; Pal, S.; Chakraborty, C. Targeted enhancement of electrochromic memory in Fe (II) based metallo-supramolecular polymer using molybdenum disulfide quantum dots. *Sol. Energy Mater. Sol. Cells* **2022**, *236*, 111487. [CrossRef]
66. Meng, Y.; Li, Z.; Liu, Z. Enhanced electrochromic properties of inorganic–organic tungsten oxide and Prussian blue core–shell film. *J. Mater. Sci. Mater. Electron.* **2022**, *33*, 24995–25005. [CrossRef]

67. Tang, Y.; Xiao, Y.; Qiao, H.; Qi, X. Enhanced Performance in Electrochromic Devices with High-contrast and Long-term Stability via Synergistic Effect of Cl-/NO_3-Dual-anion Electrolyte. *J. Electroanal. Chem.* **2022**, *928*, 117040. [CrossRef]
68. Nad, S.; Jana, R.; Datta, A.; Malik, S. Fully Organic Electroactive Monomers for Electrochromic Behaviors having High Coloration Efficiency and Long Cycle Stability towards Flexible Solid-State Electrochromic Device. *J. Electroanal. Chem.* **2022**, *918*, 116484. [CrossRef]